Description of the low-lying levels in ^{112,114}Cd

K. Heyde,* P. Van Isacker,† M. Waroquier, and G. Wenes
Institute of Nuclear Physics, Proeftuinstraat 86, B-9000 Gent, Belgium

M. Sambataro
Kernfysisch Versneller Instituut, Groningen, The Netherlands
(Received 31 December 1981)

Starting from a simplified model, treating proton two-particle two-hole excitations in interaction with low-lying quadrupole vibrational configurations, we calculate the low-lying levels in even-even ^{112,114}Cd. We also present configuration mixing calculations within the framework of the interacting boson model. Both approaches give a good description of the quintuplet of levels occurring below $E_x \cong 1.5$ MeV in ^{112,114}Cd (energy spectra and a detailed account of $E2$ and $E0$ decay properties). Finally, we point out some similarities between both approaches and try to interpret the interacting boson model mixing parameters in terms of shell-model quantities (two-body matrix elements and single-particle energies).

[NUCLEAR STRUCTURE Collective excitations in ^{112,114}Cd; shell-model intruder states; interacting boson model configuration mixing.]

I. INTRODUCTION

The energies and decay properties of the four lowest excited states ($J_i^\pi = 2_1^+$, 0_2^+, 2_2^+, and 4_1^+) of ^{112}Cd and ^{114}Cd ($Z=48$) are known to agree qualitatively with the spherical quadrupole vibrational model. This simple picture, however, is strongly disturbed by the occurrence of low-lying extra $J_i^\pi = 0_3^+$ and 2_3^+ levels forming, together with the normal two-phonon triplet, a quintuplet of states.[1,2] The structure of these extra states is not well understood as yet. According to certain authors,[3–6] some levels in even-even Cd nuclei could have a deformed character, thus having deformations larger than those of the ground state. Meyer and Peker[6] pointed towards possible γ softness in explaining a low-lying $J_i^\pi = 0_3^+$ three-phonon level. All of these explanations, however, remain speculative without the support of detailed calculations.

In this article, we would like to stress the importance of particle-hole excitation across the $Z=50$ proton closed shell in order to generate shell-model intruder states that can explain the salient features of the even-even ^{112,114}Cd nuclei. Near the $Z=50$ closed proton shell, odd-mass nuclei such as $_{49}$In (Refs. 7–9) and $_{51}$Sb (Refs. 10–12) exhibit rotational-like bands on top of an intrinsic $\frac{1}{2}^+$ [431] and $\frac{9}{2}^+$ [404] orbital, respectively. In order to account for all low-lying levels in these nuclei, proton particle-hole (p-h) excitations across the $Z=50$ closed proton shell have to be introduced, thereby providing an explanation for the observed bands on top of the $J^\pi = \frac{1}{2}^+$ and $\frac{9}{2}^+$ levels in In and Sb, respectively.[9–12] Recently, experimental evidence for the observation of excited $J^\pi = 0^+$ states in even-even $_{50}$Sn (Refs. 13–17) and Cd (Refs. 6 and 18–20) isotopes became available. These levels are strongly excited via (τ,n) two-proton transfer reaction studies,[21] thus suggesting the importance of incorporating proton 2p-2h excitations in explaining all low-lying levels in the even-even ^{112,114}Cd nuclei. Therefore, in Sec. II, we suggest to explain the quintuplet of levels as a mixing of the normal, quadrupole two-phonon excitation with proton 2p-2h excitations across the $Z=50$ closed proton shell. A similar approach has been suggested to serve as an explanation for $J^\pi = 0^+$ excited states and the $\Delta J = 2$ quasirotational bands in even-even Sn nuclei.[22,23] In Sec. III we discuss a related approach, introducing 2p-2h excitations in an approximate way, in the framework of the interacting boson model (IBM). In Sec. IV the results of both calculations are compared to experimental data.

II. PROTON TWO-PARTICLE TWO-HOLE EXCITATIONS

Without discussing in too much detail the formalism of how to introduce proton 2p-2h excitations in the particle-core coupling model (see Refs. 22 and 23), we will indicate the main steps and approximations made.

A general Hamiltonian, describing the interacting system of vibrational excitations coupled to a few fermion degrees of freedom, can be written as:

$$H=\sum_{\lambda\mu} b^{\dagger}_{\lambda\mu}b_{\lambda\mu}(\hbar\omega_{\lambda}+\tfrac{1}{2})+\sum_{a}\epsilon_a c^{\dagger}_{\alpha}c_{\alpha}-\sum_{\substack{\alpha\beta\\ \lambda\mu}}\left[\frac{\pi}{2\lambda+1}\right]^{1/2}\xi_{\lambda}\hbar\omega_{\lambda}\langle\alpha\,|\,Y_{\lambda\mu}\,|\,\beta\rangle[b^{\dagger}_{\lambda\mu}+(-1)^{\mu}b_{\lambda-\mu}]c^{\dagger}_{\alpha}c_{\beta}$$
$$+\tfrac{1}{4}\sum_{\alpha\beta\gamma\delta}\mathscr{V}_{\alpha\beta\gamma\delta}c^{\dagger}_{\alpha}c^{\dagger}_{\beta}c_{\delta}c_{\gamma}+V_{\text{Coulomb}}\,, \tag{2.1}$$

where the first and second terms describe the unperturbed energy of the quadrupole vibrations and fermions, respectively. Here, $\hbar\omega_2$ denotes the quadrupole phonon energy and ϵ_a the single-particle (-hole) energy. The third term describes the particle (-hole)-core coupling interaction with ξ_2 as the coupling strength (see Refs. 24 and 25 for its definition); the fourth term describes the residual fermion interaction. Also the Coulomb contribution for proton p-h residual interactions is included.

The nuclear wave function describing possible proton 2p-2h excitations in the even-even Cd nuclei can now be expanded as:

$$|\,i;JM\rangle=\sum c^{i}(NR;J)\,|\,NR;JM\rangle+\sum d^{i}\{(p_1p_2)J_p[(h_1h_2)J_h,NR]I;J\}$$
$$\times\,|\,(p_1p_2)J_p[(h_1h_2)J_n\otimes NR]I;JM\rangle\,, \tag{2.2}$$

where $N(R)$ denotes the number (angular momentum) of the quadrupole vibrational excitations, and p_1,p_2 (h_1,h_2) the proton-particle (-hole) configurations, i.e., $1g_{7/2}$, $2d_{5/2}$, $2d_{3/2}$, $3s_{1/2}$, $1h_{11/2}$, and $1g_{9/2}{}^{-1}$, $2p_{3/2}{}^{-1}$, $2p_{1/2}{}^{-1}$, $1f_{5/2}{}^{-1}$, respectively. Whenever summation indices are *not* written below the summation symbol [see Eq. (2.2)] we imply summation over quantum numbers that occur in both the expansion coefficients (c^i,d^i) and the basis configurations $|\cdots\rangle$ (except the total angular momentum J). The expansion coeffficients (c^i,d^i) are obtained by diagonalizing the nuclear Hamiltonian (2.1) within the basis discussed above.

Instead of carrying out the full calculation immediately, we proceed in different steps in order to obtain better insight in the final results.

(i) In a first step, only a particular part of the nuclear Hamiltonian is diagonalized (i.e., that part H' only containing the single-hole energy, the collective quadrupole vibrations of the Cd nuclei, and the hole-core and hole-hole residual interactions) in order to obtain a description of the Pd eigenstates. Thereby, we solve the secular equation

$$H'\,|\,k;IM\rangle=\omega(I,k)\,|\,k;IM\rangle \tag{2.3}$$

with

$$|\,k;IM\rangle=\sum a^{k}[(h_1h_2)J_h,NR;I]$$
$$\times\,|\,(h_1h_2)J_h\otimes NR;IM\rangle\,, \tag{2.4}$$

where $\omega(I,k)$ gives the energy spectrum (describing the Pd nuclei) and $a^k(\ldots)$ are the expansion coefficients. In our calculations, the wave functions (2.4) only serve as an intermediate step to build more complicated configurations.

(ii) In a second step, we couple the proton $2p$ configurations with the eigenfunctions (2.4) and obtain, as a new basis, the collective vibrational configurations $|\,NR;JM\rangle$, and the proton $2p$-Pd coupled configurations $|\,(p_1p_2)J_p\otimes Ik;JM\rangle$. The wave function (2.2) can therefore be transformed into the more transparent form:

$$|\,i;JM\rangle=\sum c^{i}(NR;J)\,|\,NR;JM\rangle$$
$$+\sum l^{i}[(p_1p_2)J_p,Ik;J]$$
$$\times\,|\,(p_1p_2)J_p\otimes Ik;JM\rangle\,. \tag{2.5}$$

This wave function is obtained by solving the secular equation corresponding with the full Hamiltonian (2.1) [see Eq. (2.7) or Ref. 23 for full details]. Since many ($\pm 200-300$) proton $2p$-Pd core coupled configurations constitute the second part of the

wave function (2.5), a still more transparent representation for describing the wave function can be obtained. Diagonalizing within the proton $2p$-Pd core coupled configuration space only, bands with $\Delta J=2$ spin sequence are obtained. The particular wave functions are obtained as

$$|\,\mathrm{rot}(i);JM\rangle=\sum r^i[(p_1p_2)J_p,Ik;J]\times|\,(p_1p_2)J_p\otimes Ik;JM\rangle\ , \quad (2.6)$$

for $i=1, 2,\ldots N$, where N denotes the dimension of the $2p$-Pd core coupled configuration space and rot stands for rotational, owing to its apparent similarities with collective, rotational energy spectra for the lowest bands. One should, however, be cautious in interpreting the label i for classifying energy eigenvalues $E^i(\mathrm{rot};J)$ obtained from

$$H\,|\,\mathrm{rot}(i);JM\rangle=E^i(\mathrm{rot};J)\,|\,\mathrm{rot}(i);JM\rangle\ , \quad (2.7)$$

and take into account the remarks of Ref. 23 (Sec. II A). Moreover, in the following discussions (Sec. III), we will use "rotational-like..." for excitations corresponding to the lowest bands obtained within the $2p$-Pd core coupled subspace. Finally, the wave function of Eq. (2.5) becomes

$$|\,i;JM\rangle=\sum c^i(NR;J)\,|\,NR;JM\rangle+\sum_j s^i[\mathrm{rot}(j)]\,|\,\mathrm{rot}(j);JM\rangle\ . \quad (2.8)$$

In this representation, the possible mixing of low-lying quadrupole vibrations and other collective degrees of freedom (rotational-like) is clearly expressed in terms of the amplitudes c^i and s^i.

Calculations have been carried out for ^{112,114}Cd. In these nuclei, most evidence for a quintuplet of levels near $E_x\simeq 1.5$ MeV exists. The following parameters have been used:

(i) For the nucleon-nucleon interaction $\mathcal{V}_{\alpha\beta\gamma\delta}$, we use a surface delta interaction (SDI) with strength $G=25/A$ MeV (Ref. 26).

(ii) For the Coulomb interaction, only the direct term is considered, which becomes for the diagonal proton p-h configurations almost state independent and equal to -0.25 MeV. The nondiagonal terms are generally small.[27] The importance of the attractive Coulomb interaction for proton 2p-2h excitation was already pointed out earlier by Flynn and Kunz[28] since the nuclear residual p-h matrix elements are almost negligible (-0.1 to 0.1 MeV).

(iii) The hole-Cd core and particle-Pd core coupling strengths ξ_2 have been obtained from the known $B(E2;2_1^+\rightarrow 0_1^+)$ value in Cd and Pd, respectively.[29] They are given in Table I, as well as the quadrupole phonon energy $\hbar\omega_2$, taken as the excitation energy $E_x(2_1^+)$ of the first excited $J^\pi=2^+$ state.

(iv) Unperturbed values for the lowest proton 2p-2h excitations, i.e., $2(\epsilon_{1g_{7/2}}-\epsilon_{1g_{9/2}})$, are taken from proton separation energies[30] as $2[S_p(Z=50)-S_p(Z=51)]$. The relative single-particle (-hole) energies obtained from a recent study of odd-mass In nuclei[9,31] are also used here (see Table I).

In order to carry out the calculations discussed above, certain approximations in the calculation of the matrix elements of the Hamiltonian (2.1) within the basis described by Eqs. (2.5) or (2.8) have been considered. We use the approximations outlined in Eqs. (2.12) and (2.13) of Ref. 23 in the calculation of the residual matrix elements. Thereby, numerical efforts are simplified without loss of the general physics content of the model.

The electromagnetic $E2$ and $E0$ decay properties are calculated using the transition operators as discussed in Ref. 23. The proton effective charge used was $e_p^{\mathrm{eff}}=1.5e$ and the experimental $B(E2;2_1^+\rightarrow 0_1^+)$ values for Cd and Pd nuclei, respectively, are used to determine the collective $E2$ transition strength.

TABLE I. Parameters in approach A (see Sec. II) (using the explicit introduction of proton 2p-2h excitations) used to calculate energy spectra of ^{112,114}Cd. All parameters given are in MeV, except for the dimensionless coupling strengths ξ_2,ξ_3.

$\hbar\omega_2$(Cd)	0.617
$\hbar\omega_2$(Pd)	0.375
ξ_2(Cd)	6.0
ξ_2(Pd)	12.0
$\tilde{\epsilon}_{2p_{1/2}}$	0.7
$\tilde{\epsilon}_{2p_{3/2}}$	1.3
$\tilde{\epsilon}_{1f_{5/2}}$	2.1
$\epsilon_{1g_{7/2}}$	0.0
$\epsilon_{2d_{5/2}}$	0.2
$\epsilon_{2d_{3/2}}$	2.6
$\epsilon_{3s_{1/2}}$	2.95
$\epsilon_{1h_{11/2}}$	2.10
$2(\epsilon_p-\epsilon_h)$	9.49±0.04
ΔE_h	2.39±0.01

III. CONFIGURATION MIXING IN THE INTERACTING BOSON MODEL

The neutron-proton interacting boson model (*n-p* IBM) proposes a description of a nucleus in terms of a system of neutron and proton interacting bosons.[32,33] The number of bosons of each type is computed as half the number of the corresponding nucleons outside the closed shells or, if the shell is more than half-filled, as half the complementary holes. A normal *n-p* IBM calculation of the ^{112}Cd (^{114}Cd) nucleus would imply $N_\pi=1$ proton bosons and $N_\nu=7$ ($N_\nu=8$) neutron bosons. In the presence of proton 2p-2h excitations, however, two protons are excited across the closed $Z=50$ shell. This introduces an additional hole boson in the $Z=28-50$ shell and a particle boson in the $Z=50-82$ shell. Therefore, three active proton bosons can be associated with this particular type of configuration. Both the normal configuration and the one containing a proton 2p-2h excitation are shown in Fig. 1 for ^{114}Cd. The configuration mixing, for simplicity, does not distinguish between bosons being in different major shells and describes both the configurations within the standard scheme of the *n-p* IBM. Moreover, it introduces an appropriate term in the Hamiltonian which mixes the two types of configurations. The Hamiltonian used in these calculations is the usual *n-p* IBM Hamiltonian,[34-36]

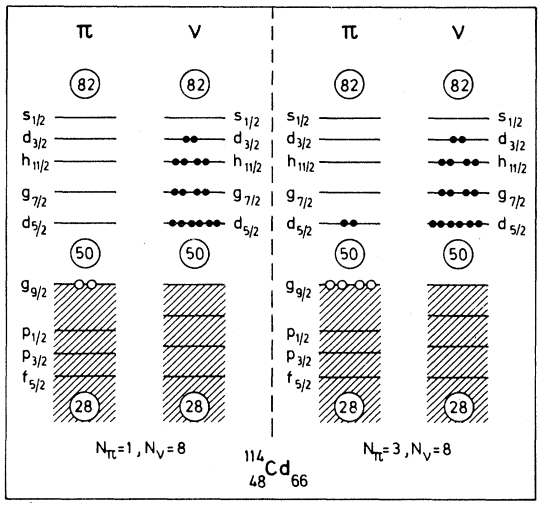

FIG. 1. A schematic representation of the particular $N_\pi=1$ and $N_\pi=3$ configuration in the *n-p* IBM configuration mixing calculation, in ^{114}Cd. The distribution of particles over the available single-particle orbitals as well as the ordering of levels are drawn in order to guide the eye.

$$H=\epsilon_\pi d_\pi^\dagger\cdot\tilde{d}_\pi+\epsilon_\nu d_\nu^\dagger\cdot\tilde{d}_\nu+V_{\pi\pi}+V_{\nu\nu}+\kappa Q_\pi\cdot Q_\nu+M_{\pi\nu}\,, \tag{3.1}$$

where

$$V_{\rho\rho}=\sum_{L=0,2,4}\tfrac{1}{2}c_{L\rho}(2L+1)^{1/2}\times[(d_\rho^\dagger d_\rho^\dagger)^{(L)}(\tilde{d}_\rho\tilde{d}_\rho)^{(L)}]^{(0)}\,, \tag{3.2}$$

and

$$Q_\rho=(s_\rho^\dagger\tilde{d}_\rho+d_\rho^\dagger s_\rho)^{(2)}+\chi_\rho(d_\rho^\dagger\tilde{d}_\rho)^{(2)}\,, \tag{3.3}$$

with $\rho\equiv\pi,\nu$. Moreover, the Majorana term $M_{\pi\nu}$ reads

$$M_{\pi\nu}=-\sum_{\kappa=1,3}2\xi_\kappa(d_\pi^\dagger d_\nu^\dagger)^{(\kappa)}\cdot(\tilde{d}_\pi\tilde{d}_\nu)^{(\kappa)}+\xi_2(d_\pi^\dagger s_\nu^\dagger-s_\pi^\dagger d_\nu^\dagger)^{(2)}\cdot(\tilde{d}_\pi s_\nu-s_\pi\tilde{d}_\nu)^{(2)}\,. \tag{3.4}$$

Here, ϵ_π and ϵ_ν stand for the energies of the proton and neutron bosons, respectively, and for simplicity, we take $\epsilon_\pi=\epsilon_\nu$. The interactions among identical bosons are expressed by $V_{\pi\pi}$, $V_{\nu\nu}$, and the term $\kappa Q_\pi\cdot Q_\nu$ denotes the quadrupole-quadrupole interaction acting between neutron and proton bosons. Finally, $M_{\pi\nu}$ is the Majorana operator which effects the energy of those states which are not fully symmetric in the neutron-proton degree of freedom. The mixing Hamiltonian used is the one suggested in Refs. 37 and 38,

$$H_{\rm mix}=\alpha(s_\pi^\dagger s_\pi^\dagger+s_\pi s_\pi)^{(0)}+\beta(d_\pi^\dagger d_\pi^+ +\tilde{d}_\pi\tilde{d}_\pi)^{(0)}\,. \tag{3.5}$$

One has to remark that the quadrupole operator in Sec. II, Eq. (2.1), describing the particle-core coupling, has the standard expression obtained from the residual interaction between collective surface quadrupole vibrations and single-particle degrees of freedom.[24,25] Using the IBM description [see Eq. (3.3)], a term that is proportional to $(d^\dagger\tilde{d})^{(2)}$ in the collective quadrupole operator results. Therefore, differences between both approaches do occur. We think, however, that the underlying physics allows one to draw a close parallelism between both approaches, as will be discussed in more detail in Secs. III and IV.

The calculations are carried out in two steps. In *the first step,* the Hamiltonian (3.1) is diagonalized for each configuration separately in the usual basis[36]

$$|[(d_\pi)^{n_{d_\pi}}(L_\pi\phi_\pi)(s_\pi)^{N_\pi-n_{d_\pi}}(d_\nu)^{n_{d_\nu}}(L_\nu\phi_\nu)(s_\nu)^{N_\nu-n_{d_n}}]^{(L)}|0\rangle\ , \tag{3.6}$$

where ϕ_π,ϕ_ν denote the additional quantum numbers which characterize the states uniquely. *In the second step,* $H+H_{\rm mix}$ is diagonalized in a basis provided by the lowest eigenstates of the $N_\pi=1$ and $N_\pi=3$ configurations. In this step, an energy Δ is also introduced which, added to the eigenvalues of the configurations with $N_\pi=3$, represents the extra energy needed to excite such a configuration. (This latter value is related to

$$2(\epsilon_p-\epsilon_h)-\{[S_p(Z=50)-S_p(Z=49)]-[S_p(Z=52)-S_p(Z=51)]\}$$

in the approach discussed in Sec. II; see also the Appendix. Here $S_p(Z)$ denotes proton separation energy.)

All the important parameters used in the calculations are given in Table II. The parameters of the Hamiltonian (3.1) are close to the ones used in calculations for nearby nuclei.[34,35] The parameters of the mixing Hamiltonian α and β are kept equal and constant and, for Δ, a value of 5.45 MeV is used. A short discussion on a possible relation between the parameters α, β, and Δ, and the parameters of the approach of Sec. II, is given in the Appendix. The electromagnetic transitions are evaluated using an $E2$ operator of the form

$$T(E2)=e_1(Q_{\pi_1}+Q_{\nu_1})+e_3(Q_{\pi_3}+Q_{\nu_3})\ , \tag{3.7}$$

where $Q_\rho(\rho\equiv\nu,\pi)$ are the operators (3.3), the subscripts 1 and 3 refer to the two configurations, and e_j $(j=1,3)$ are the boson effective charges. If only relative $B(E2)$ values are considered, only the ratio e_3/e_1 is important. In the calculations presented here a ratio $e_3/e_1=1.6$ was considered.

IV. STUDY OF ^{112,114}Cd NUCLEI

A. Energy spectra

The energy spectrum as calculated using the approach in which proton 2p-2h excitations are included explicitly (approach A) is shown in Fig. 2 for ^{114}Cd, up to an excitation energy of $E_x\simeq4$ MeV (left part of the spectrum). On the right hand side of the same figure, we show the result of the IBM mixing calculations. In the latter case, only eight levels of each J^π value have been calculated ($J^\pi=0^+$, 2^+, 4^+, 6^+, 8^+, 10^+, and 12^+). We are aware of the fact that, already at $E_x\simeq2$ MeV, the experimental level density becomes much higher owing to the neglect, in approach A, of explicit neutron excitations in obtaining the final spectrum. The thickened lines contain important components within the $2p$-Pd core coupled configuration space (A) or within the $N_\pi=3$ configuration space (approach B) and generate a kind of rotational-like band. The experimental data are taken from Ref. 20.

For the rest of the discussion, however, we will mainly concentrate on the quintuplet of states near $E_x\simeq1.5$ MeV. The wave functions describing the lowest $J^\pi=0^+$, 2^+, 4^+, and 6^+ levels show large mixing and in many cases it becomes difficult to assign a main component to the state (see Tables III and IV).

A more detailed comparison of the calculated level scheme with the experimental data for ^{112,114}Cd [also containing the $B(E2)$ reduced transition probabilities; see Sec. IV B] is given in Fig. 3.

Before describing in detail the energy spectra, obtained from the *n-p* IBM mixing calculation (ap-

TABLE II. Parameters in approach B (see Sec. III) (the neutron-proton IBM configuration mixing calculations) used to calculate energy spectra of ^{112,114}Cd. All parameters are in MeV, except for χ_ν and χ_π (dimensionless). The parameters for the configurations with $N_\pi=1$ and $N_\pi=3$ are denoted explicitly.

		$\epsilon_\pi=\epsilon_\nu$	κ	χ_ν	χ_π	$C_{0\nu}$	$C_{2\nu}$	ξ_2	$\alpha=\beta$	Δ
$^{112}_{48}Cd_{64}$	$N_\pi=1$	0.9	−0.15	−0.9	−0.2	−0.22	−0.08	0.06	0.08	5.45
	$N_\pi=3$	0.4	−0.2035	−0.9		−0.22	−0.08			
$^{114}_{48}Cd_{66}$	$N_\pi=1$	0.83	−0.14	−0.9	−0.2	−0.19	−0.045	0.06	0.08	5.45
	$N_\pi=3$	0.40	−0.19	−0.9		−0.19	−0.045			

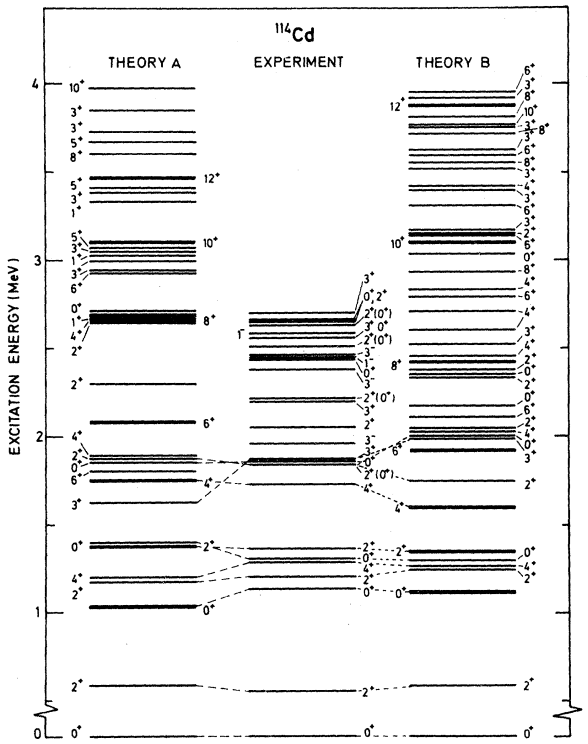

FIG. 2. Comparison of the experimental level scheme of ^{114}Cd (Ref. 47) with the theoretical calculated energy spectrum, using both approach A and B. The levels drawn with a thickened line have their main components within the 2*p*-Pd core coupled configuration space (A) [see also Eq. (2.8)] or within the $N_\pi=3$ configuration space, for approach B.

proach B), we will discuss the main contributions from the Hamiltonian (3.1) in producing the quintuplet of states near $E_x\simeq 1.5$ MeV. In Fig. 4, we show in a schematic, although detailed way, how the $N_\pi=3$ configuration (dashed lines) interacts with the $N_\pi=1$ configuration (full lines). Only levels necessary to explain the quintuplet of states near $E_x\simeq 1.5$ MeV are shown. In this figure, one clearly observes how the proton-neutron $\kappa Q_\pi\cdot Q_\nu$ interaction can lower the $N_\pi=3$ configuration owing to the much larger binding energy relative to the energy of the $N_\pi=1$ configuration. Finally, in the region $-0.15<\kappa<-0.20$ MeV, the mixing Hamiltonian (3.5) can connect both subsystems and induce the necessary configuration mixing to lead to good agreement with experiment at $\kappa=-0.19$ MeV for ^{114}Cd. A simple estimate of the excitation energy of the intruder 2p-2h configurations in even-even Cd nuclei can be obtained from the IBM mixing calculations. Neglecting the change in binding energy as a function of the neutron boson number in the $N_\pi=1$ configurations, one can calculate in an approximate way the relative excitation energy for the $N_\pi=3$ configurations. Since the major terms contributing to the energy are given via the Hamiltonian

$$H_{(N_\pi=3,N_\nu)}\cong\Delta+\kappa Q_\pi\cdot Q_\nu\ , \tag{4.1}$$

the expectation value, for a particular nucleus $N_\pi=3$, N_ν, becomes

$$E_{(N_\pi=3,N_\nu)}\cong\Delta+\bar{\kappa}N_\pi N_\nu\ . \tag{4.2}$$

TABLE III. Wave functions for the lowest $J^\pi=0^+$, 2^+, 4^+, and 6^+ levels in ^{114}Cd, using approach A (see Sec. II). The amplitudes of the wave functions, using the expansion of Eq. (2.8) are given (only amplitudes ≥ 0.10). The notation $|1\rangle$, $|2\rangle$, $|3\rangle$, $|4\rangle$ and $|\bar{1}\rangle$, $|\bar{2}\rangle$, $|\bar{3}\rangle$, $|\bar{4}\rangle$ stands for the lowest four vibrational and rotational-like configurations, respectively, compatible with the angular momentum of the particular level.

	$\|1\rangle$	$\|2\rangle$	$\|3\rangle$	$\|4\rangle$	$\|\bar{1}\rangle$	$\|\bar{2}\rangle$	$\|\bar{3}\rangle$	$\|\bar{4}\rangle$
$\|0_1^+\rangle$	0.86	0.11			0.44			
$\|0_2^+\rangle$	−0.34	0.65	−0.06		0.61			
$\|0_3^+\rangle$	−0.12	−0.41	−0.72		0.36		0.34	
$\|0_4^+\rangle$	−0.20	−0.52	0.55		0.55			
$\|2_1^+\rangle$	−0.76				−0.60	−0.15		
$\|2_2^+\rangle$	0.32	0.71			−0.42	0.43		
$\|2_3^+\rangle$	0.47	−0.45	−0.33		−0.61	−0.16		
$\|4_1^+\rangle$	0.68				0.70			
$\|4_2^+\rangle$	−0.63	−0.16			0.69			
$\|4_3^+\rangle$		0.94			0.16			
$\|6_1^+\rangle$	−0.40				0.90	−0.11		
$\|6_2^+\rangle$	−0.81				−0.42	−0.37		

TABLE IV. See caption of Table III, using approach B (see Sec. III) for ^{112}Cd and for ^{114}Cd. Here the notation $|1\rangle$, $|2\rangle$, $|3\rangle$, $|4\rangle$ and $|\bar{1}\rangle$, $|\bar{2}\rangle$, $|\bar{3}\rangle$, $|\bar{4}\rangle$ stands for the lowest four $N_\pi=1$ and $N_\pi=3$ eigenstates, respectively, compatible with the angular momentum of the particular level.

				^{112}Cd				
		$N_\pi=1$, $N_\nu=7$				$N_\pi=3$, $N_\nu=7$		
	$\|1\rangle$	$\|2\rangle$	$\|3\rangle$	$\|4\rangle$	$\|\bar{1}\rangle$	$\|\bar{2}\rangle$	$\|\bar{3}\rangle$	$\|\bar{4}\rangle$
$\|0_1^+\rangle$	0.99							
$\|0_2^+\rangle$		0.72			0.69			
$\|0_3^+\rangle$		−0.69			0.71			
$\|0_4^+\rangle$			0.98			0.17	−0.10	
$\|2_1^+\rangle$	0.99							
$\|2_2^+\rangle$		0.86			−0.50			
$\|2_3^+\rangle$		−0.50	−0.16	−0.10	−0.84			
$\|2_4^+\rangle$			−0.98		0.16			
$\|4_1^+\rangle$	0.97				0.23			
$\|4_2^+\rangle$	0.23	−0.15			−0.96			
$\|4_3^+\rangle$		−0.98			0.15			
$\|6_1^+\rangle$	0.62				−0.78			
$\|6_2^+\rangle$	0.78				0.62			
				^{114}Cd				
		$N_\pi=1$, $N_\nu=8$				$N_\pi=3$, $N_\nu=8$		
	$\|1\rangle$	$\|2\rangle$	$\|3\rangle$	$\|4\rangle$	$\|\bar{1}\rangle$	$\|\bar{2}\rangle$	$\|\bar{3}\rangle$	$\|\bar{4}\rangle$
$\|0_1^+\rangle$	0.99							
$\|0_2^+\rangle$		0.71			0.70			
$\|0_3^+\rangle$		0.70			−0.71			
$\|0_4^+\rangle$			0.98			0.13	−0.10	
$\|2_1^+\rangle$	0.99							
$\|2_2^+\rangle$		0.84			0.53			
$\|2_3^+\rangle$		0.54	0.16		−0.82			
$\|2_4^+\rangle$			0.98		0.18			
$\|4_1^+\rangle$	0.97				−0.23			
$\|4_2^+\rangle$	0.22	−0.15			0.96			
$\|4_3^+\rangle$		0.98			0.15			
$\|6_1^+\rangle$	0.63				−0.78			
$\|6_2^+\rangle$	0.77				0.62			

In Fig. 5, we show the particular dependence for the even-even Cd nuclei, using $\Delta=5.45$ MeV and $\bar{\kappa}=-0.20$ MeV.

In Fig. 6, we show, for the particular value of $\kappa=-0.19$ MeV, the unperturbed energy spectrum (putting $\alpha=\beta=0$) of ^{112}Cd. One observes that different levels will be mixed strongly by the Hamiltonian (3.5), especially the $N_\pi=1$ (0_2^+,2_2^+) and the $N_\pi=3$ (0_1^+, 2_1^+) levels. The wave functions obtained are given in Table IV and the energy spectra are compared with the experimental data in Figs. 7 and 8.

In comparing both approaches, one observes that the energy splitting of the quintuplet is larger in approach A. This same feature is reflected in the larger mixing of the wave functions in approach A (compare Tables II and IV). The difference is related to the small values of the α and β mixing parameters in approach B whereas, in approach A, the coupling matrix elements are related to the SDI two-body pairing and quadrupole matrix elements (see the Appendix). This results in much larger matrix elements affecting the final states in a much more profound way.

B. Electromagnetic transitions ($E2$,$E0$)

Before discussing in detail the $E2$ decay properties of the ^{112,114}Cd quintuplet of levels near

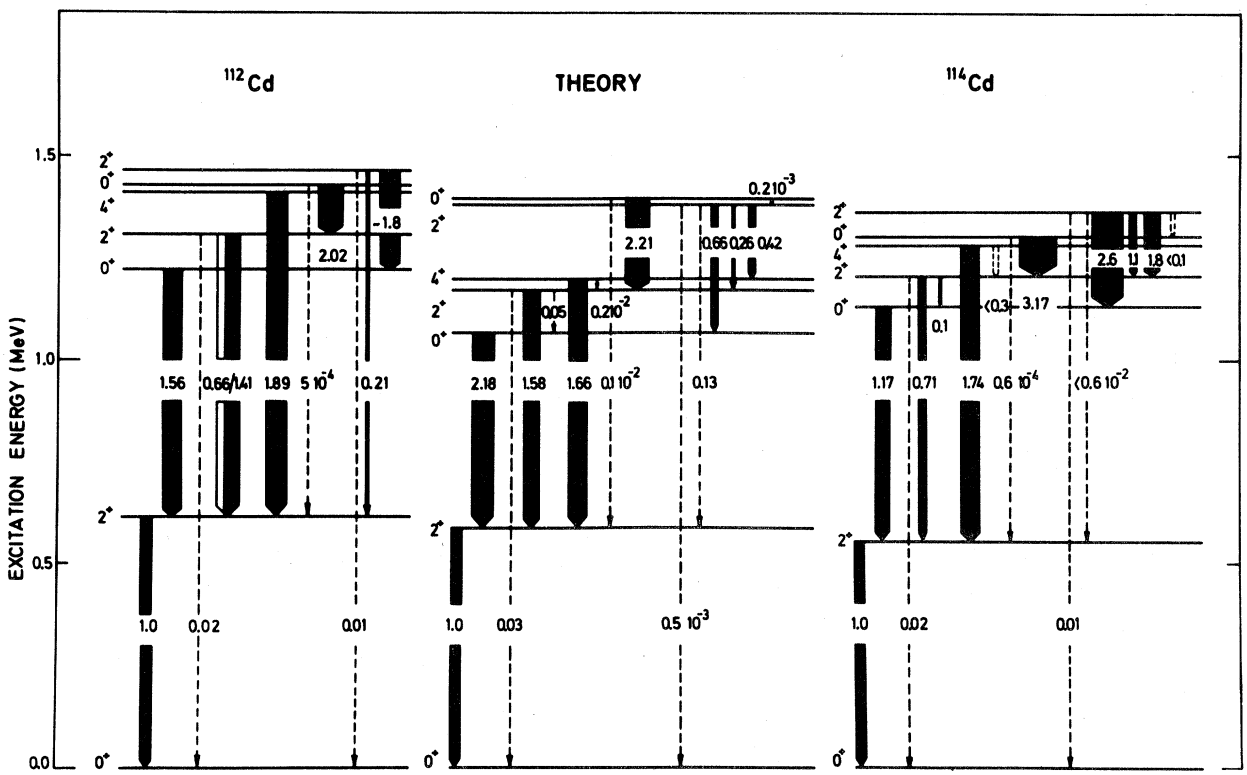

FIG. 3. Comparison of the relative $B(E2)$ values [relative to $B(E2; 2_1^+ \rightarrow 0_1^+)$] between low-lying levels ($E_x < 1.5$ MeV) in ^{112}Cd and ^{114}Cd (experimental data are averaged values of data from Refs. 1, 2, 18–20, and 39–47) with the calculated values using approach A. The thickness of the arrows is proportional to the $B(E2)$ values and serves to guide the eye.

$E_x \simeq 1.5$ MeV we indicate that the experimental data are taken from Refs. 1, 2, 18–20, and 39–47, and that averaged $B(E2)$ values are used when different experimental data exist (except for the $J_i^\pi = 4_1^+$ lifetime where the measurement of Akkerman *et al.*[40] is discarded).

The $E2$ decay pattern of the quintuplet of states in ^{112}Cd and in ^{114}Cd is remarkably similar. Therefore, we will discuss the general features at the same time. Extensive comparison with the experiment is carried out in both approaches A (see Fig. 2) and B (see Figs. 7 and 8) [$B(E2)$ values relative to $B(E2, 2_1^+ \rightarrow 0_1^+)$ are given]. Notice that in the case of ^{112}Cd, fewer data on $B(E2)$ values between levels near $E_x \cong 1.5$ MeV exist as compared with ^{114}Cd, the latter nucleus being studied in a more detailed way (Refs. 20 and 47).

First of all, it is evident that, although the $J_i^\pi = 0_2^+$, 2_2^+, and 4_1^+ levels show a remarkable vibrational structure (apart from the presence of the intruder $J^\pi = 0^+$ and 2^+ states), non-negligible deviations in the $E2$ decay are observed. In ^{114}Cd, the $B(E2; 0_2^+ \rightarrow 2_1^+)$ and $B(E2; 2_2^+ \rightarrow 2_1^+)$ are approximately half of the pure vibrational intensity rule. On the contrary, the $J^\pi = 4_1^+$ state follows the normal trend rather well. In the IBM configuration mixing calculations, such an anomalous behavior can be explained as follows. As is seen in Table IV, the $J_i^\pi = 0_2^+$, 0_3^+ and 2_2^+, 2_3^+ states are strongly admixed. Moreover, since the intruder $J^\pi = 0^+$ and 2^+ states originate from configurations with $N_\pi = 3$, the above $J_i^\pi = 0_2^+$, 0_3^+ and 2_2^+, 2_3^+ states will have large components both in the configurations with $N_\pi = 1$ and $N_\pi = 3$. Since the $J_i^\pi = 2_1^+$ state mainly belongs to the $N_\pi = 1$ configuration space and since the $E2$ operator cannot connect levels belonging to different subsystems, it follows that the $N_\pi = 1$ component of the wave function of the $J_i^\pi = 0_2^+$ and 2_2^+ states will mainly contribute to the decay towards the $J_f^\pi = 2_1^+$ state. In this IBM calculation, the particular component is also 50% (see Table IV) and will produce a decay rate which is in satisfactory agreement with the experimental data (see also Table V where the contributions to the $E2$

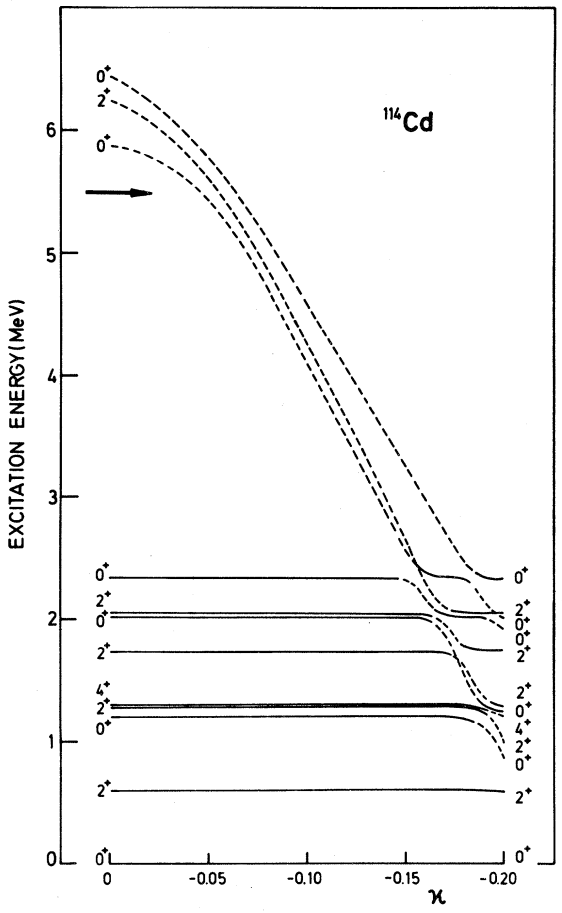

FIG. 4. The dependence of the lowest $J^\pi=0^+$, 2^+, 4^+ $N_\pi=1$ levels (full lines) and the lowest $J^\pi=0^+$, 2^+ $N_\pi=3$ levels (dashed lines) in ^{114}Cd as a function of the proton-neutron quadrupole-quadrupole force strength κ acting in the $N_\pi=3$ space. The change in character of the line representing a particular level reflects the change in the wave function.

matrix element in the different subsystems $N_\pi=1$ and $N_\pi=3$ are given for some important transitions). To this respect, the approach A gives $B(E2;\ 0_2^+\rightarrow 2_1^+)$ and $B(E2;\ 2_2^+\rightarrow 2_1^+)$ which are somewhat larger. The cause is to be found in the fact that the $J_i^\pi=2_1^+$ wave function contains large admixtures of the intruder $2p$-Pd core coupled configurations (see Table III) and, therefore, the contribution to the $B(E2;\ 0_2^+\rightarrow 2_1^+)$ value resulting from the transitions within the $2p$-Pd core coupled configuration space is too important (see also Table VI, where the separate $E2$ contributions adding up to the total $E2$ matrix element are given).

Another very interesting phenomenon is the decay of the $J_i^\pi=0_3^+$ level. This state decays preferen-

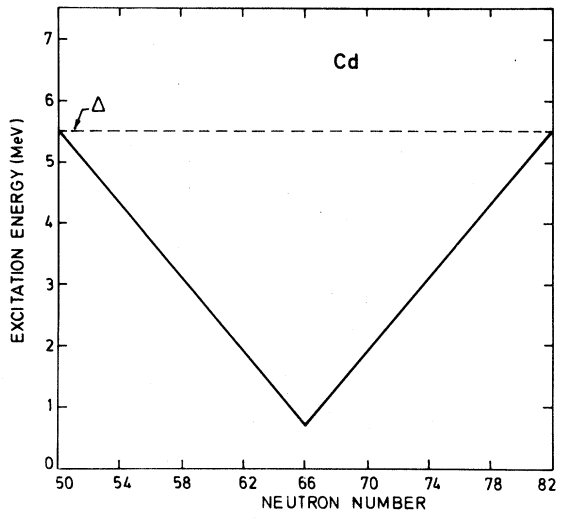

FIG. 5. The neutron dependence of proton 2p-2h intruder state excitation energies as estimated from the IBM approach. The dashed line shows the unperturbed energy Δ.

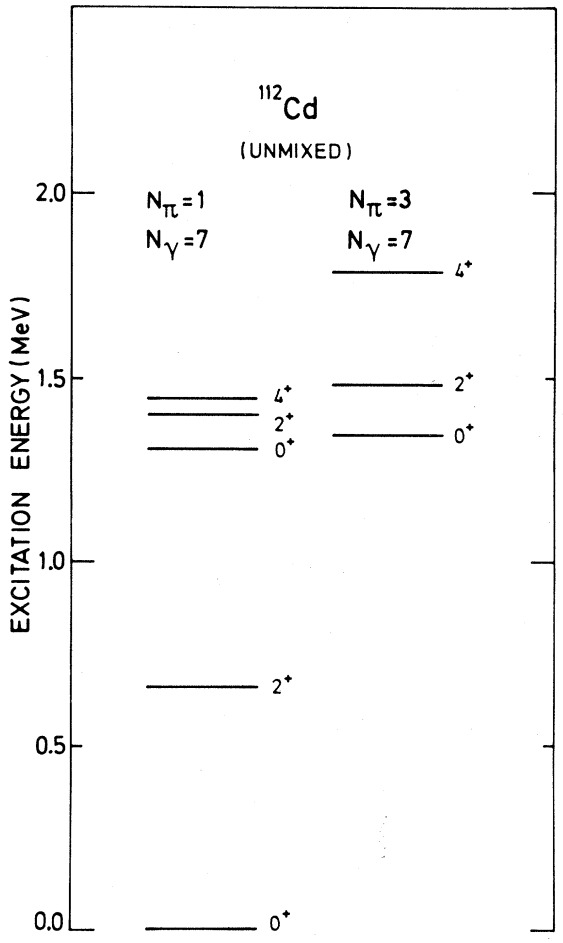

FIG. 6. Part of the unperturbed $N_\pi=1$ and $N_\pi=3$ level scheme, using the parameters of Table II for ^{112}Cd. Here, we have assumed $\alpha=\beta=0$.

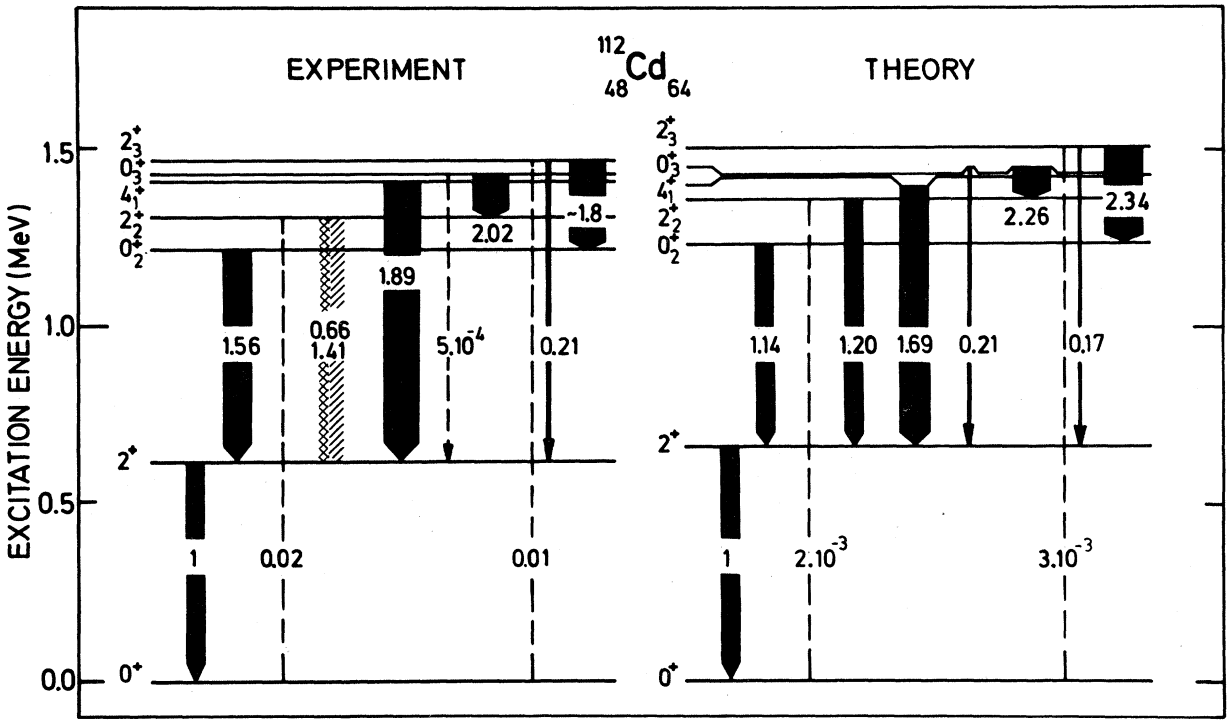

FIG. 7. See caption of Fig. 3 but for approach B and for ^{112}Cd. Only the theoretical $B(E2)$ values are drawn which compare to a measured $B(E2)$ value.

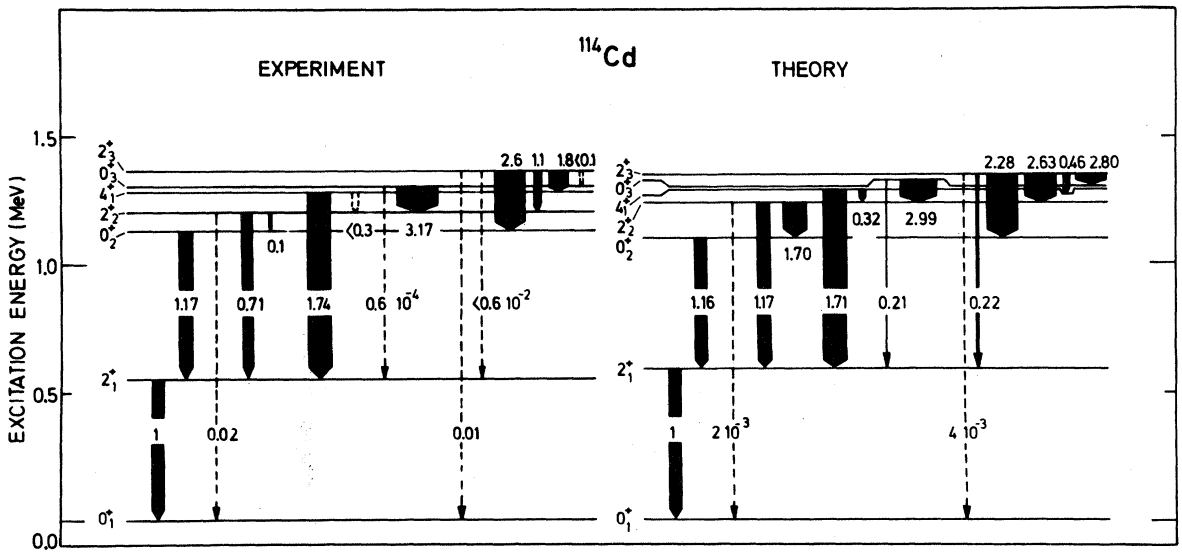

FIG. 8. See caption of Fig. 3 but for approach B and for ^{114}Cd.

TABLE V. Partial (for the separate $N_\pi=1$ and $N_\pi=3$ configuration spaces) and total $E2$ matrix elements in approach B (using arbitrary units) for some important transitions. The upper (lower) row numbers refer to the ^{112}Cd (^{114}Cd) nucleus, respectively.

	$\langle J_f^\pi \|\|M(E2)\|\|J_i^\pi\rangle$		
$J_i^\pi \to J_f^\pi$	$E2$ ($N_\pi=1$)	$E2$ ($N_\pi=3$)	$E2$ (Total)
$0_3^+ \to 2_1^+$	2.75	−1.20	1.55
	2.97	−1.29	1.68
$\to 2_2^+$	1.97	−7.06	−5.09
	2.04	−8.33	−6.29
$0_2^+ \to 2_1^+$	2.39	1.23	3.62
	2.58	1.35	3.93
$\to 2_2^+$	2.39	6.84	9.23
	2.49	8.12	10.61
$2_3^+ \to 0_2^+$	0.45	−12.02	−11.57
	0.53	−12.80	−12.27
$\to 0_3^+$	0.36	12.42	12.78
	0.44	13.19	13.63

tially into the $J_f^\pi=2_2^+$ level rather than to the $J_f^\pi=2_1^+$ level, the latter transition being almost forbidden. When studying the separate $E2$ contribution for these $E2$ transitions, we observe that for both approaches, large $E2$ matrix elements result in both the normal and intruder configuration space (see Tables V and VI). It is, however, the particular feature of constructive and destructive interference between two strongly collective $E2$ decay amplitudes (normal quadrupole vibrational and rotational-like) which is able to explain this very peculiar decay pattern. This interference pattern is even more pronounced in the approach taking proton 2p-2h excitations explicitly into account. The same interference mechanism was necessary to explain the $E2$ and $E0$ decay properties in $^{112-118}$Sn nuclei.[22,23]

Finally, the large $B(E2; 2_3^+ \to 0_2^+)$ value is also predicted in both approaches A and B. The partial contribution to the $E2$ matrix element are again shown in Tables V and VI.

In order to indicate the possibility to go beyond the quintuplet of states near $E_x \simeq 1.5$ MeV, we have calculated within both approaches for ^{114}Cd the $E2$ decay properties from the next higher group of $J_i^\pi=4_2^+$, 2_4^+, 0_4^+, and 3_1^+ levels. The comparison is carried out with experimental data from Schreckenbach *et al.*[20] In these data, the most intense $E2$ transition was normalized to 100 for the relative $B(E2)$ values, assuming moreover pure $E2$ gamma decay. Here again a satisfactory agreement results (see Table VII).

The quadrupole moments $Q(2_1^+)$ have been determined in an accurate way[45,48,49] and are

TABLE VI. Partial $E2$ matrix elements for the vibrational [Coll. (I)] and rotational-like [Coll. (II)] configuration space, in approach A for some important transitions in ^{114}Cd. Also the total $E2$ matrix elements are given. The units are e b.

	$\langle J_f^\pi \|\|M(E2)\|\|J_i^\pi\rangle$		
$J_i^\pi \to J_f^\pi$	Coll (I)	Coll (II)	Total
$0_3^+ \to 2_1^+$	18.6	−17.3	1.3
$0_3^+ \to 2_2^+$	−32	−20.5	−52.5
$0_2^+ \to 2_1^+$	−7.1	−45.4	−52.5
$0_2^+ \to 2_2^+$	−3.2	−14.0	−17.2
$2_3^+ \to 0_2^+$	−13.1	−51.5	−64.6
$2_3^+ \to 0_3^+$	−15.2	16.2	1.0

TABLE VII. The experimental relative $B(E2)$ values for the $J_i^\pi=4_2^+$, 2_4^+, 0_4^+, and 3_1^+ initial states in ^{114}Cd. The most intense $E2$ transition (assuming pure $E2$ decay, marked with an asterisk) is normalized to 100. Comparison with calculations of both approach A and B is given.

$J_i^\pi \to J_f^\pi$	2p-2h	*n-p* IBM	Exp.
$4_2^+ \to 2_1^+$	16	0.04	0.5
$\to 2_2^+$	72	48	29
$\to 4_1^+$	60	6	20*
$\to 2_3^+$	100	100	100
$2_4^+ \to 0_1^+$	2.3	0.4	0.2
$\to 2_1^+$	2.3	0.12	3.5*
$\to 0_2^+$	77	14	48
$\to 2_2^+$	20	5	6.2*
$\to 0_3^+$	35	144	38
$\to 2_3^+$	100	100	100*
$0_4^+ \to 2_1^+$	1.3	0.3	13
$\to 2_2^+$	0.5	113	<5
$\to 2_3^+$	100	100	100
$3_1^+ \to 2_1^+$	1.3	1	2.7*
$\to 2_2^+$	100	100	100*
$\to 4_1^+$	36	47	41*
$\to 2_3^+$	22	42	1.4*

-0.39 ± 0.08 and -0.36 ± 0.8 e b in ^{112}Cd and ^{114}Cd, respectively. The calculated values, in the configuration mixing IBM are -0.34 and -0.36 e b, respectively. Approach A gives a value of -0.25 e b. Thus, calculation A still underestimates the quadrupole moment in the even-even ^{112,114}Cd nuclei. In approach A, the proton 2p-2h excitations induce correlations which act coherently with the pure quadrupole vibrational contribution (the latter being only -0.10 e b) so as to build up a quadrupole moment of sizeable magnitude. In the IBM mixing calculation (see Table IV) the $J_i^\pi=2_1^+$ wave function is mainly $N_\pi=1$. Here also $Q(N_\pi=1, 2_1^+)$ and $Q(N_\pi=3, 2_1^+)$ act coherently.

Using the calculated $B(E2)$ and $B(M1)$ values in approach A (effective gyromagnetic factors have been used: $g_R=Z/A$, $g_l=1$, and $g_s=2.79$ and 4.20), the half-lives for the $J_i^\pi=2_1^+$, 2_2^+, 2_3^+, 0_2^+, 0_3^+, and 4_1^+ levels have been calculated (using the experimental E_γ deexcitation energies). Partial $T_{1/2}$ $(E2)$, $T_{1/2}$ $(M1)$, and total $T_{1/2}$ values are given in Table VIII and compared with the available experimental data. From the table, one observes the following features:

(i) The $2_2^+ \to 2_1^+$ transition contains about 30% $M1$ admixture. This calculated value is in good agreement with the experimental results of Schreckenbach *et al.*[20]

(ii) The $2_3^+ \to 2_1^+$ has an $E2/M1$ ratio of 50%. The results of Schreckenbach *et al.*[20] give $M1$ as the most important component, and with much less $E2$ admixture ($<2.5\%$).

(iii) The $T_{1/2}(0_3^+)$ value is always calculated too small. This quantity, however, is very sensitive to the $B(E2; 0_3^+ \to 2_1^+)$, which results from destructive interference between two large numbers and therefore cannot be calculated very reliably.

Finally, we discuss some $E0$ decay rates (Table IX) in both ^{112,114}Cd (Refs. 18 and 47). The calculations were carried out using the same $E0$ operator and methods as outlined in Ref. 23. Also $E0$ transitions between $J^\pi \neq 0^+$ states are calculated and are shown to contribute in a non-negligible way to the decay of a particular level. The theoretical results give a satisfactory reproduction of most of the experimental data although the $0_2^+ \to 0_1^+$ and the $0_3^+ \to 0_1^+$ states are somewhat too high. With respect to the structure of the 0_2^+ and 0_3^+ states, we note that the situation in ^{112,114}Cd (and especially in ^{114}Cd) is considerably different from that seen in ^{116}Sn (Ref. 23). In the latter nucleus, in fact, a very intense $0_3^+ \to 0_2^+$ transition was observed ($\rho^2 \times 10^3 \simeq 100$) which was explained as being due to a mixing of largely different equilibrium shapes for both $J_i^\pi=0_2^+$ and 0_3^+. From our wave functions (see Table II) one indeed can see that the structure of the

TABLE VIII. Partial $T_{1/2}$ ($E2$), $T_{1/2}$ ($M1$) (using $g_s=2.79$ and $g_s=4.2$, respectively) and total $T_{1/2}$ half-lives (using $g_s=2.79$) in ps compared with the experimental data for ^{112}Cd and ^{114}Cd.

$J_i^\pi \to J_f^\pi$	$T_{1/2}(E2)$	$T_{1/2}(M1)$		$T_{1/2}$	$T_{1/2}$(Exp)
^{112}Cd					
$2_1^+ \to 0_1^+$	4.9			4.9	6.0
$2_2^+ \to 2_1^+$	1.8	7.0	7.0	1.0	1.7
$\to 0_1^+$	3.9				
$4_1^+ \to 2_1^+$	0.83			0.83	0.9
$2_3^+ \to 0_1^+$	120				
$\to 2_1^+$	7.6	4.3	3.8	2.5	2.9
$0_2^+ \to 2_1^+$	2.5			2.5	4.2
$0_3^+ \to 2_1^+$	890			890	1900
^{114}Cd					
$2_1^+ \to 0_1^+$	8.1			8.1	9.1
$2_2^+ \to 2_1^+$	2.4	8.5	8.5	1.9	2.8
$\to 0_1^+$	5.8				
$4_1^+ \to 2_1^+$	1.3			1.3	1.4
$2_3^+ \to 0_1^+$	173			3.1	3.8
$\to 2_1^+$	10	5.1	4.5		
$0_2^+ \to 2_1^+$	3.2			3.2	6.6
$0_3^+ \to 2_1^+$	1380			1380	5500

0_2^+ and 0_3^+ states is different from what was obtained in the ^{116}Sn core (Table III of Ref. 23) where orthogonal combinations of only two configurations [$|20;0\rangle$ and $|\text{rot}(1);0^+\rangle$] occur.

In the IBM mixing calculation, also $E0$ transitions can be calculated. If, as one would expect, only protons contribute to these transitions, the most general one-body $E0$ operator becomes

$$T(E0)=a\hat{N}_\pi+b(d_\pi^\dagger\tilde{d}_\pi)^{(0)}\,, \tag{4.3}$$

where the operator $\hat{N}_\pi\equiv(s_\pi^\dagger s_\pi+d_\pi^\dagger\cdot\tilde{d}_\pi)$ counts the number of proton bosons. In a normal n-p IBM calculation, the first term can be neglected because it is diagonal in the eigenstates of the Hamiltonian (3.1). In a mixing calculation, however, this term has to be included because the mixed states have components in the configuration spaces with both $N_\pi=1$ and $N_\pi=3$ different for each level (consequently different states have different eigenvalues of $\hat{N}_\pi$). However, since the coefficients a and b of the operator (4.3) are expected to be different in the two subspaces $N_\pi=1$ and $N_\pi=3$, the calculation of $E0$ transitions would imply a number of parameters comparable to that of the well known $E0$ transitions indicated in Table IX. Therefore, no definitive conclusions can be reached about these $E0$ transitions in the IBM approach.

TABLE IX. Theoretical $E0$ decay matrix elements using approach A ($\rho^2\times10^3$), compared to some important experimental $E0$ transition rates in ^{112}Cd and ^{114}Cd.

$J_i^\pi \to J_f^\pi$	$E0$ rates ($\rho^2\times10^3$) ^{112}Cd	^{114}Cd	Theory
$0_2^+ \to 0_1^+$	37	27	77
$0_3^+ \to 0_1^+$	0.48	1.5	4.6
$0_3^+ \to 0_2^+$	8.1	0.4	1.1
$2_2^+ \to 2_1^+$		$\langle 8$	2
$2_3^+ \to 2_1^+$		61	26
$2_3^+ \to 2_2^+$		34	3

V. CONCLUSION

In this study, we have tried to point out the importance of proton 2p-2h excitations across the $Z=50$ closed proton shell in order to describe in detail the low-lying quintuplet of levels in even-even ^{112,114}Cd nuclei. Within a simple model (approach A), containing proton 2p-2h excitations interacting with quadrupole vibrational excitations of the underlying Cd core, we were able to show how intruder states can occur at low excitation energy and in which way they modify the standard vibrational

two-phonon multiplet structure as well as its $E2$ decay properties.

Starting from the neutron-proton IBM, and approximating the proton 2p-2h configurations via the addition of two extra s or d bosons, a configuration mixing calculation was carried out for ^{112,114}Cd (approach B). This approach gives results similar to the former one (approach A).

Extensive comparison between both approaches and the existing experimental data was carried through. One of the most interesting features, i.e., the very peculiar decay pattern of the 0_3^+ level is well reproduced through constructive interference between two strong collective $E2$ decay amplitudes: a vibrational and a rotational-like amplitude. This same feature is also observed in the adjacent doubly-even ^{116}Sn nucleus.

ACKNOWLEDGMENTS

The authors are indebted to Professor F. Iachello for much help and inspiration on the problem of intruder states within the IBM. They are grateful to Dr. A. E. L. Dieperink, Dr. B. Barrett, Dr. J. Wood, Dr. P. Duval, Dr. O. Scholten, Dr. R. Casten, Dr. A. Bäcklin, and Dr. K. Schreckenbach for many discussions, provoking questions, and use of data prior to publication. Two of the authors (P.V.I. and M.W.) are indebted to the Nationaal Fonds voor Wetenschappelyk Onderzoek (NFWO), (G.W.) to the Instituut voor Wetenschappelyk Onderzoek in Nijverherd en Landbouw (IWONL), and (K.H.) to the InterUniversitaire Instituut voor Kernwetonschappen (IIKW) for financial support. One of the authors (M.S.) is grateful to the Stichting Fundamenteel Onderzock der Materie (FOM), and the Foundazione A. Della Riccia, Italy for financial support and to the Kernfysisch Versneller Instituut (KVI) for its hospitality.

APPENDIX: RELATION BETWEEN THE TWO APPROACHES A AND B

From the discussion of Secs. II and III, it becomes clear that both approximations to describe the quintuplet of levels in ^{112,114}Cd nuclei are related to each other. Exciting a proton pair across the $Z=50$ closed shell will form proton 2p-2h configurations. Since the excited pairs most likely occur as $J^\pi=0^+$ or 2^+ angular momentum coupled pairs, the analogy with the mixing term in the n-p IBM approach, see Eq. (3.5), containing the creation (annihilation) of a pair of s or d proton bosons is immediately clear.

In order to relate the parameters of both approaches, two-body shell-model matrix elements can be put equal to the corresponding n-p IBM matrix elements. In particular, information on the mixing parameters α and β should result.

The basic coupling matrix element connecting both parts of the wave function of (2.5) (see also the Appendix of Ref. 23) becomes

$$L[N'R';(p_1p_2)J_p,Ik;J]\equiv\langle N'R';J\mid H\mid(p_1p_2)J_p,Ik;J\rangle\ , \tag{A1}$$

or, using the explicit form of the $\mid k;IM\rangle$ wave function of Eq. (2.4), one gets

$$L=-\sum_{\substack{h_1h_2J_h\\NR}}(-1)^{J_p+R+I}(\hat{I}/\hat{R})a^k((h_1h_2)J_h,NR;I)\langle p_1p_2,J_p\mid V\mid h_1h_2,J_h\rangle\delta_{J_pJ_h}\delta_{NN'}\delta_{RR'}\ . \tag{A2}$$

When lifting a $J^\pi=0^+$ coupled pair across the $Z=50$ closed shell, one has $J_h=J_p=0$ whereas for $J^\pi=2^+$ coupled pairs, one has $J_h=J_p=2$. Specifying now the interaction matrix element with the $\mid N'=0,\ R'=0;0\rangle$ vibrational, zero phonon state, and only considering pair states in the summation, i.e., $h_1\equiv h_2\equiv h$, one gets

$$L(N'=0,\ R'=0;(p)^2J_p=0,0_1^+;0)\simeq-\sum_h a^k[(h)_0^2,N=0,R=0;0]\langle(p)_0^2\mid V\mid(h)_0^2\rangle \tag{A3}$$

and

$$L(N'=0,\ R';(p)^2J_p=2;2_1^+;0)\simeq-\sum_h\sqrt{5}a^k[(h)_2^2,N=0,\ R=0;2]\langle(p)_2^2\mid V\mid(h)_2^2\rangle\ , \tag{A4}$$

for the 0^+ and 2^+ pair creation coupling matrix elements, respectively. Therefore, the ratio of the coefficients α and β in the *n-p* IBM mixing Hamiltonian could be taken proportional to the ratio of a typical pairing and quadrupole two-body matrix elements. Using, as discussed in Sec. II, the SDI force, we can write

$$\frac{\beta}{\alpha} \cong \frac{\langle (p)_2^2 \mid V \mid (h)_2^2 \rangle}{\langle (p)_0^2 \mid V \mid (h)_0^2 \rangle} = \frac{\begin{pmatrix} j_p & j_p & 2 \\ \frac{1}{2} & -\frac{1}{2} & 0 \end{pmatrix} \begin{pmatrix} j_h & j_h & 2 \\ \frac{1}{2} & -\frac{1}{2} & 0 \end{pmatrix}}{\begin{pmatrix} j_p & j_p & 0 \\ \frac{1}{2} & -\frac{1}{2} & 0 \end{pmatrix} \begin{pmatrix} j_h & j_h & 0 \\ \frac{1}{2} & -\frac{1}{2} & 0 \end{pmatrix}} . \tag{A5}$$

For typical orbitals near $Z=50$, taking $j_h \equiv 1g_{9/2}$ and $j_p \equiv 1g_{7/2}$, $2d_{5/2}$, an average ratio $\beta/\alpha=0.25$ results.

In order to determine both α and β, we will have to equate a typical matrix element in both approaches. Therefore, we have to transform from the basis $|(p_1p_2)J_p,Ik;JM\rangle$ into the more appropriate basis $|\text{rot}(i);JM\rangle$ of Eq. (2.6) in order to have matrix elements conform with the mixing matrix elements in the *n-p* IBM calculation where $N_\pi=1$ and $N_\pi=3$ eigenstates (obtained after separate *n-p* IBM calculations) occur. This transformation [Eq. (2.6)] results from a diagonalization of the nuclear Hamiltonian (2.1) within the $2p$-Pd core-coupled configuration space only. The latter eigenstates $|\text{rot}(i);JM\rangle$ with energies $E^i(\text{rot};J)$ [Eq. (2.7)] are now in some way equivalent to the $N_\pi=3$ IBM eigenstates, and so we are able to equate corresponding matrix elements. A typical vibrational, rotational-like coupling matrix element becomes

$$\tilde{L}(N'R';\text{rot}(i);J) \equiv \langle N'R';J \mid H \mid \text{rot}(i);J \rangle = \sum_{\substack{p_1p_2J_p \\ Ik}} r^i[(p_1p_2)J_p,Ik,J]\langle N'R' \mid H \mid (p_1p_2)J_p,Ik;J\rangle . \tag{A6}$$

Within the latter representation [see Eq. (2.8)] of the wave function, the final secular equation reads (fully analogous with the $N_\pi=1$, $N_\pi=3$ IBM mixing Hamiltonian secular equation),

$$\begin{vmatrix} N_2\hbar\omega_2\delta_{NN'}\delta_{RR'} & \tilde{L}(\text{rot}(i),NR;J) \\ \tilde{L}(NR;\text{rot}(i);J) & E^{(i)}(\text{rot};J) \end{vmatrix} . \tag{A7}$$

In specifying the matrix element (A6) to the particular case of coupling of the $J^\pi=0^+$ states, we consider the zero-phonon vibrational configuration $|N'=0;\ R'=0,0\rangle$ (equivalent to the $N_\pi=1$ lowest $J^\pi=0^+$ state) and the lowest rotational-like $J^\pi=0^+$ state obtained from $|\text{rot}(i);0^+\rangle$ (equivalent to the $N_\pi=3$ lowest $J^\pi=0^+$ state). Making use of the expansion (A6), one gets

$$\tilde{L}(N'=0,R'=0;\text{rot}(1);0^+) = -0.40 \text{ MeV} .$$

The same matrix element, within *n-p* IBM mixing calculation becomes

$$M(N_\pi=1,N_\pi=3) \equiv \langle 0_1^+(N_\pi=1,N_\nu=8) \mid \alpha(s_\pi s_\pi)+\beta(\tilde{d}_\pi\tilde{d}_\pi)^{(0)} \mid 0_1^+(N_\pi=3,N_\nu=8)\rangle . \tag{A8}$$

We now assume that the $N_\pi=1$ lowest $J^\pi=0^+$ state is the zero-phonon state, i.e.,

$$|0_1^+(N_\pi=1,N_\nu=8)\rangle = |n_{d_\pi}=0,n_{d_\nu}=0\rangle , \tag{A9}$$

and, furthermore, we use the following expansion of the $N_\pi=3$ lowest $J^\pi=0^+$ state

$$|0_1^+(N_\pi=3,N_\nu=8)\rangle = 0.084\,|n_{d_\pi}=0,n_{d_\nu}=0\rangle + 0.203\,|n_{d_\pi}=0,n_{d_\nu}=2\rangle + 0.189\,|n_{d_\pi}=1,n_{d_\nu}=1\rangle + 0.052\,|n_{d_\pi}=2,n_{d_\nu}=0\rangle , \tag{A10}$$

which is obtained from the diagonalization of the n-p IBM Hamiltonian in the $N_\pi=3$, $N_\nu=8$ basis. Calculating further the matrix element (A8), one obtains the value

$$M(N_\pi=1,\ N_\pi=3)=0.206\alpha+0.074\beta\ . \quad \text{(A11)}$$

Assuming a wave function for $|0_1^+(N_\pi=1,\ N_\nu=8)\rangle$ which also includes components with $n_{d_\pi}+n_{d_\nu}=2$, one obtains the following improved expression for the matrix element (A8) in terms of α and β as

$$M(N_\pi=1,N_\pi=3)=0.448\alpha+0.155\beta\ . \quad \text{(A12)}$$

Using now the ratio $\beta/\alpha=0.25$ and the value of the shell-model matrix element of -0.40 MeV, one gets

$$\alpha=-0.82\ \text{MeV},\ \beta=-0.21\ \text{MeV}\ . \quad \text{(A13)}$$

The difference between the fitted values $\alpha=\beta=0.08$ MeV in the IBM approach and the calculated values of (A13) is quite important. A possible explanation can result from different causes:

(i) The fact that $\alpha>\beta$, in approach A seems to reflect the importance of exciting 0^+ pairs over 2^+ pairs with respect to the boson description,

(ii) For each different coupling matrix element within the shell-model approach, calculating (A6) will result in different values of the α and β parameters that are needed to fit the corresponding IBM matrix element precisely. Averaging over all matrix elements of the Hamiltonian (2.1) for each J^π value will result in an important lowering with respect to the values given in (A13). For the $J^\pi=0^+$ matrix, average values of α, and β, when taking the lowest ten basis configurations, results in $\bar{\alpha}=-0.25$ MeV; $\bar{\beta}=-0.16$ MeV.

From the shell-model calculations, as already stated in Sec. II B of Ref. 23, there is a very specific dependence on J for the $\tilde{L}$-coupling matrix elements:

(i) For growing J^π, the $\tilde{L}$-coupling matrix elements become on the average smaller.

(ii) For a particular J^π, the larger the "unperturbed energy difference" of interacting J^π states, the smaller the interaction matrix element, thus

$$\tilde{L}(N=1,R=2;\text{rot}(1);2^+)>\tilde{L}(N=2,R=2,\text{rot}(2);2^+)>\ldots>\tilde{L}(N=3,R=2;\text{rot}(3);2^+)\ .$$

The parameter Δ is related to the proton 2p-2h energy, lowered by the proton 2h and proton 2p pairing energy ΔE_h and ΔE_p, respectively. Empirical estimates can be made (see also Table I) for the $Z=50$ Sn mass region thus, one can approximately equate:

$$\Delta\cong E_{\text{unp}}=2(\epsilon_p-\epsilon_h)-\Delta E_p-\Delta E_h\ , \quad \text{(A14)}$$

or

$$\Delta\cong 2[S_p(Z=50)-S_p(Z=51)]-[S_p(Z=50)-S_p(Z=49)]-[S_p(Z=52)-S_p(Z=51)]\ . \quad \text{(A15)}$$

Using the Wapstra and Boss mass tables,[30] one gets values for Δ of 5.19, 5.37, 5.18, and 4.77 MeV for ^{118,116,114,112}Sn respectively; thus, the value of $\Delta=5.45$ MeV, as chosen here for the study of ^{112,114}Cd, is not unreasonably large. In the n-p IBM mixing calculation, contributions of the nuclear Hamiltonian (3.1) to the $N_\pi=1$ and $N_\pi=3$ energies are such that for *no* proton-neutron interaction in the latter $N_\pi=3$ system [$\kappa(N_\pi=3)=0$], an effective spacing of $\Delta E=5.9$ MeV between the lowest $J^\pi=0^+$ levels from both the $N_\pi=1$ and $N_\pi=3$ subsystems results (see also Fig. 4).

In the shell-model approach, contributions from the nuclear Hamiltonian (2.1) into the configuration space of 2p-Pd core coupled configurations (still for $\xi_2=0$ but *including* the $\tilde{L}$-mixing matrix elements) give an additional shift to E_{unp} to enlarge this value to almost 6 MeV (see also Figs. 2 and 3 of Ref. 23).

From the discussion given above, a relation between ξ_2 and κ becomes clear. In the n-p IBM calculations, the term $\kappa Q_\pi\cdot Q_\nu$ brings the $N_\pi=3$ system down, relative to the $N_\pi=1$ system, owing to a very large binding energy gain via the quadrupole interaction acting among proton and neutron bosons (see Fig. 4). In the shell-model approach (see Sec. II) no distinction between proton and neutron degrees of freedom is made. Since we couple explicitly proton shell-model degrees of freedom (proton 2p-2h excitations) to collective quadrupole core vibrations (unspecified) via the interaction Hamiltonian

$$H_{\text{int}}=-\left[\frac{\pi}{5}\right]^{1/2}\xi_2\hbar\omega_2 Y_2(\hat{r}_\pi)\cdot(b_2^+ +\tilde{b}_2)\ , \quad \text{(A16)}$$

we cannot discriminate between the particular

proton-neutron contribution relative to the proton-proton energy gain. One knows, however, that in single-closed shell nuclei, i.e., Sn nuclei, the lowest $J^{\pi}=2^{+}$ quadrupole vibrational excitation is mainly built out of neutron quasiparticle configurations[50–52] so that one can expect that the largest contribution to $H_{\rm int}$ comes from the proton-neutron interaction, and can write approximately

$$H_{\rm int}\simeq\left[\frac{\pi}{5}\right]^{1/2}\xi_2\hbar\omega_2 Y_2(\hat{r}_\pi)\cdot[b_2^{+}(\nu)+\tilde{b}_2(\nu)]\ . \tag{A17}$$

*Also at: Rŷksuniversitert Gent, STVS, & LEKF, Krŷgslaan 271, 59-B900 Gent, Belgium.

†Present address: Instituto de Fisica, Universidad Nacional Autonoma de Mexico Apdo. Postal, 20-364, Mexico 20, D. F.

[1]L. K. Peker, Nucl. Data Sheets 29, 587 (1980).

[2]H. J. Kim, Nucl. Data Sheets 16, 107 (1975).

[3]R. K. Sheline, Rev. Mod. Phys. 32, 1 (1960).

[4]A. Bäcklin, N. E. Holmberg, and G. Bäckstrom, Nucl. Phys. 80, 154 (1966).

[5]L. von Bernus, V. Schneider, and W. Greiner, Lett. Nuovo Cimento 6, 527 (1973).

[6]R. A. Meyer and L. Peker, Z. Phys. A 283, 379 (1977).

[7]W. Dietrich, A. Bäcklin, C. O. Lannergard, and I. Ragnarsson, Nucl. Phys. A253, 429 (1975).

[8]K. Heyde, M. Waroquier, P. van Isacker, and H. Vincx, Nucl. Phys. 292, 237 (1977).

[9]K. Heyde, M. Waroquier, and R. A. Meyer, Phys. Rev. C 17, 219 (1978).

[10]A. K. Gaigalas, R. E. Shroy, G. Schertz, and D. B. Fossan, Phys. Rev. Lett. 35, 555 (1975).

[11]J. Bron, W. H. A. Hesselink, H. Bedet, H. Verheul, and G. Vanden Berghe, Nucl. Phys. A279, 365 (1977).

[12]P. van Isacker, M. Waroquier, H. Vincx, and K. Heyde, Nucl. Phys. A292, 125 (1977).

[13]J. Bron, W. H. A. Hesselink, A. van Poelgeest, J. J. A. Zalmstra, M. J. Uitzinger, H. Verheul, K. Heyde, M. Waroquier, P. van Isacker, and H. Vincx, Nucl. Phys. A318, 335 (1979).

[14]J. Bron, Ph.D. thesis, Vrye Universiteit Amsterdam, 1978 (unpublished).

[15]J. Kantele, R. Julin, M. Luontama, A. Passoja, T. Poikolainen, A. Bäcklin, and N. G. Johnson, Z. Phys. A 289, 157 (1979).

[16]A. Bäcklin, N. G. Jonson, R. Julin, J. Kantele, M. Luontama, A. Passoja, and T. Poikolainen, Nucl. Phys. A351, 490 (1981).

[17]N. G. Jonson, A. Bäcklin, J. Kantele, R. Julin, M. Luontama, and A. Passoja Nucl. Phys. A371, 333 (1981).

[18]R. Julin, J. Kantele, M. Luontama, A. Passoja, T. Poikolainen, A. Bäcklin, and N. G. Jonson, Z. Phys. A 296, 315 (1980).

[19]D. D. Warner, R. F. Casten, M. L. Stelts, and K. Heyde, Proceedings of the International Conference on Nuclear Physics, Berkeley, 1980, LBL Report No. LBL-11118.

[20]K. Schreckenbach A. Mheemed, G. Barreau, T-von Egidy, H. R. Faust, H. G. Börner, R. Brissot, M. L. Stelts, K. Heyde, P. Van Isader, M. Waroquier, and G. Wenes, Phys. Lett. (to be published).

[21]H. W. Fielding. R. E. Anderson, C. D. Zafiratos, D. A. Lind, F. E. Cecil, H. H. Wieman, and W. P. Alford, Nucl. Phys. A281, 289 (1977).

[22]G. Wenes, P. van Isacker, M. Waroquier, K. Heyde, and J. van Maldeghem, Phys. Lett. 98B, 398 (1981).

[23]G. Wenes, P. van Isacker, M. Waroquier, K. Heyde, and J. van Maldeghem, Phys. Rev. C 23, 2291 (1981).

[24]K. Heyde and P. J. Brussaard, Nucl. Phys. A104, 81 (1967).

[25]V. Paar, Nucl. Phys. A211, 29 (1973).

[26]L. S. Kisslinger and R. A. Sorensen, Rev. Mod. Phys. 35, 853 (1963).

[27]A. E. L. Dieperink, H. P. Leenhouts, and P. J. Brussaard, Nucl. Phys. A116, 556 (1968).

[28]E. R. Flynn and P. D. Kunz, Phys. Lett. 68B, 40 (1977).

[29]C. K. Ross and R. K. Badhuri, Nucl. Phys. A196, 369 (1972).

[30]A. H. Wapstra and K. Boss, At. Data Nucl. Data Tables 19, 177 (1977).

[31]K. Heyde, M. Waroquier, and P. van Isacker, Phys. Rev. C 22, 1267 (1980).

[32]T. Otsuka, A. Arima, and F. Iachello, Nucl. Phys. A309, 1 (1978).

[33]O. Scholten, Ph.D. thesis, University of Groningen, 1980 (unpublished).

[34]G. Puddu, O. Scholten, and T. Otsuka, Nucl. Phys. A348, 109 (1980).

[35]P. van Isacker and G. Puddu, Nucl. Phys. A348, 125 (1980).

[36]R. Bijker, A. E. L. Dieperink, and O. Scholten, Nucl. Phys. A344, 207 (1980).

[37]P. Duval and B. R. Barrett, Phys. Lett. 100B, 223 (1981).

[38]M. Sambataro and G. Molnar, Kernfysisch Versneller Institut Report KVI-316, 1981; Nucl. Phys. (to be published).

[39]P. H. Stelson and F. K. McGowan, Phys. Rev. 121, 209 (1961).

[40]A. F. Akkerman *et al.*, JETP Lett. 16, 899 (1963).

[41]F. K. Mc. Gowan, R. L. Robinson, P. H. Stelson, and J. L. C. Ford Jr., Nucl. Phys. 66, 97 (1965).

[42]W. T. Milner, F. K. Mc. Gowan, P. H. Stelson, R. L. Robinson, and R. O. Sayer, Nucl. Phys. A129, 687 (1969).

[43]Z. W. Grabowski and R. L. Robinson, Nucl. Phys. A206, 633 (1973).

[44]B. Fogelberg, A. Bäcklin, and J. McDonald, in Proceedings of the Conference on Problems of Vibrational Nuclei, Zagreb, 1974, Vol. II (Contributed Papers); Fizika (Zagreb) Suppl. 2. 7, 218 (1975).

[45]Z. M. Naqib, A. Christy, I. Hall, M. F. Nolan, and D. J. Thomas, J. Phys. G 3, 507 (1977).

[46]N. G. Jonson, J. Kantele, and A. Bäcklin, Nucl. Instrum. Methods 152, 485 (1978).

[47]A. M. Mheemed, K. Schreckenbach, G. Barreau, T. von Egidy, J. Valentin, H. R. Faust, H. G. Börner, R. Brissot, and M. Stelts, Contributed paper to the 4th International Symposium on Neutron Capture γ-ray Spectroscopy and Related Subjects, 1981.

[48]M. T. Esat, D. C. Kean, R. H. Spear, and A. M. Baxter, Nucl. Phys. A274, 237 (1976).

[49]W. A. Gillespie, M. W. S. Macauley, A. Johnston, E. W. Lees, and R. P. Singhal, J. Phys. G 3, L169 (1977).

[50]D. M. Clement and E. U. Baranger, Nucl. Phys. A120, 25 (1968).

[51]A. van Poelgeest, J. Bron, W. H. A. Hesselink, K. Allaart, J. J. A. Zalmstra, M. J. Uitzinger, and H. Verheul, Nucl. Phys. A346, 70 (1980).

[52]G. Bonsignori and M. Savoia, Nuovo Cimento 63A, 411 (1981).